

# Four-body continuum-discretized coupled-channels calculations

M. Rodríguez-Gallardo<sup>1,2,3</sup>, J. M. Arias<sup>2</sup>, J. Gómez-Camacho<sup>2,4</sup>, A. M. Moro<sup>2</sup>,  
I. J. Thompson<sup>5</sup>, and J. A. Tostevin<sup>6</sup>

<sup>1</sup> *IEM, CSIC, Serrano 123, 28006 Madrid, Spain*

<sup>2</sup> *Depto. FAMN, Universidad de Sevilla, Apto. 1065, 41080 Sevilla, Spain*

<sup>3</sup> *CFNUL, Universidade de Lisboa, Av. Prof. Gama Pinto 2, 1649-003 Lisboa, Portugal*

<sup>4</sup> *CNA, Av. Thomas A. Edison, 41092 Sevilla, Spain*

<sup>5</sup> *LLNL, Physical Science Directorate, P.O. Box 808, L-414, Livermore, CA 94551, USA and*

<sup>6</sup> *Department of Physics, University of Surrey, Guildford, Surrey GU2 7XH, United Kingdom*

(Dated: October 30, 2018)

The development of a continuum-bins scheme of discretization for three-body projectiles is necessary for studies of reactions of Borromean nuclei such as  ${}^6\text{He}$  within the continuum-discretized coupled-channels approach. Such a procedure, for constructing bin states on selected continuum energy intervals, is formulated and applied for the first time to reactions of a three-body projectile. The continuum representation uses the eigenchannel expansion of the three-body S-matrix. The method is applied to the challenging case of the  ${}^6\text{He} + {}^{208}\text{Pb}$  reaction at 22 MeV, where an accurate treatment of both the Coulomb and the nuclear interactions with the target is necessary.

PACS numbers: 21.45.-v, 24.50.+g, 25.60.-t, 24.10.Eq, 27.20.+n

Rapid experimental developments have made studies of the scattering and reactions of very weakly-bound systems possible in many branches of physics. Among these are the Efimov states observed in ultra-cold cesium trimers [1] and molecular triatomic systems, such as  $\text{LiHe}_2$  [2], halo nuclei [3], systems undergoing two-proton radioactivity [4], and also Bose-Einstein condensates and ultra-cold dilute gas studies. The need for novel and quantitative theoretical descriptions of the dynamics of such systems, which must include *a priori* a realistic treatment of their continuum spectra, is common to many problems. Here we discuss continuum effects in the nuclear physics context of reactions of weakly-bound halo nuclei [3, 5, 6]. The study of these systems is of special importance in nuclear physics in order to learn properties of the nucleon-nucleon interaction in the low density limit and investigate the role of pairing off the stability line. Many of these exotic nuclei play a significant role in astrophysical processes. Although the method is general, in this Rapid Communication, we will discuss reactions of the Borromean halo nucleus  ${}^6\text{He}$ , i.e. the bound three-body ( ${}^4\text{He}+n+n$ ) system with (i) no bound excited states and (ii) no bound binary sub-systems.

Due to their weak binding, halo nuclei are readily excited to the continuum (broken-up) by the differential forces exerted on the constituents through the nuclear and Coulomb interactions with a target. Theoretically, the explicit treatment of these breakup channels is difficult since the states involved are infinite in number and are not square-integrable. Hence a robust discretization and truncation scheme, to provide a finite and normalizable basis to represent the continuum, is required. The continuum-discretized coupled-channels (CDCC) method, as formulated for two-body projectiles [7, 8], uses bin states to represent the continuum. Here, the continuum spectrum is truncated at a maximum excitation energy  $\varepsilon_{\max}$  and the model space, from

the breakup threshold to  $\varepsilon_{\max}$ , is then divided into intervals, where the number and positions of the intervals can depend on the properties (e.g. resonant or non-resonant) of the continuum of the system. For each such interval, or energy bin, a representative square-integrable state is constructed as a linear superposition of the two-body scattering states in the interval. The method has been enormously successful in the description of elastic and breakup observables in reactions involving weakly-bound two-body projectiles [9, 10, 11] and has been recently extended to include core excitation [12].

Of interest here are reactions of three-body projectiles. To date, published discretized three-body projectile calculations have used a pseudostate (PS) basis [13, 14, 15, 16], accounting reasonably well for existing elastic scattering data. Based on our own experience [15] of calculations using PS bases, convergence problems were found for reactions where the Coulomb interaction plays an important role. The alternative continuum treatment using the energy bin technique within the CDCC has yet to be formulated and the present work provides this theoretical development.

To describe the three-body ground and excited continuum states of the projectile we make use of a hyperspherical harmonics (HH) expansion basis [17]. This involves use of the one radial and five angular hyperspherical coordinates,  $\rho, \alpha, \hat{x}, \hat{y}$ , obtained from the normalized Jacobi coordinates  $\mathbf{x}, \mathbf{y}$  of the three bodies [15, 17]. The quantum number set,  $\beta$ , that defines each three-body channel [15] are the hypermomentum  $K$ , the orbital angular momenta  $l_x$  and  $l_y$  in coordinates  $\mathbf{x}$  and  $\mathbf{y}$ , their total  $\mathbf{l} = \mathbf{l}_x + \mathbf{l}_y$ , the total spin  $S_x$  of the particles associated with coordinate  $\mathbf{x}$ , and the intermediate summed angular momentum  $\mathbf{j}_{ab} = \mathbf{l} + \mathbf{S}_x$ . If the spin of the third particle,  $I$ , is assumed fixed then the total angular momentum is  $\mathbf{j} = \mathbf{j}_{ab} + \mathbf{I}$  with projections  $\mu$ . Note that, for each continuum energy  $\varepsilon$  and total angular momentum  $j$ , there

will be as many independent solutions of the three-body scattering problem, as the number of outgoing channels  $\beta$  considered. These solutions can be chosen as the incoming channels  $\beta'$ , but any orthogonal combination of these could be equally valid.

Based on these total angular momentum eigenstates,  $\mathcal{Y}_{\beta j \mu}(\Omega)$  [15], where  $\Omega \equiv (\alpha, \hat{x}, \hat{y})$ , the bin wave functions are defined as

$$\phi_{n j \mu}^{\text{bin}}(\mathbf{x}, \mathbf{y}) = \sum_{\beta} R_{n \beta j}^{\text{bin}}(\rho) \mathcal{Y}_{\beta j \mu}(\Omega), \quad (1)$$

where the label  $n$  includes reference to the energy interval of the bin  $[\kappa_1, \kappa_2]$ , as well as to the set of quantum numbers  $\beta'$ . The functions  $R_{n \beta j}^{\text{bin}}(\rho)$  in Eq. (1) are the associated hyperradial wave functions,

$$\begin{aligned} R_{n \beta j}^{\text{bin}}(\rho) &\equiv R_{[\kappa_1, \kappa_2] \beta' \beta j}^{\text{bin}}(\rho) \\ &= \frac{2}{\sqrt{\pi N_{\beta' j}}} \int_{\kappa_1}^{\kappa_2} d\kappa e^{-i\delta_{\beta' j}(\kappa)} f_{\beta' j}(\kappa) R_{\beta \beta' j}(\kappa, \rho), \end{aligned} \quad (2)$$

where  $\kappa = \sqrt{2m|\varepsilon|/\hbar}$  is the momentum associated to the continuum energy  $\varepsilon$ ,  $R_{\beta \beta' j}(\kappa, \rho)$  are the continuum hyperradial wave functions with  $\delta_{\beta' j}(\kappa)$  their scattering phase shift, and  $f_{\beta' j}(\kappa)$  is a weight function with  $N_{\beta' j}$  its normalization constant. Note that for each  $j$  and three-body energy bin we must construct wave functions for all allowed incoming channels  $\beta'$ . Further, as is explicit in Eq. (1), for each  $n$  we must also construct  $R_{n \beta j}^{\text{bin}}(\rho)$  for all allowed outgoing channels  $\beta$ .

It follows that to include a large number of  $\beta'$  channels is a severe computational challenge, and that it is desirable to establish a hierarchy of the continuum states according to their importance to the reaction dynamics. In so doing, we may be able to describe scattering observables using only a selected set of states, the number of them depending on the reaction under study. To this end, we make use of the eigenstates of the multi-channel three-body S-matrix [18], or eigenchannels (EC), as follows. (i) For each  $j$  and continuum energy  $\varepsilon$ , the S-matrix in the  $\beta$  basis is diagonalized to obtain its EC, enumerated by  $\gamma$ , their corresponding eigenvalues  $\exp[2i\delta_{\gamma j}(\kappa)]$  and eigenphases  $\delta_{\gamma j}(\kappa)$ . (ii) The magnitudes of these eigenphases are used to order the EC. We will show that those EC with largest phase shifts are the most strongly coupled in the reaction dynamics, and thus a hierarchy of states can be established by such an ordering. This leads to the possibility of a truncation in the number  $n_{ec}$  of EC included and testing of the convergence with respect to this number.

Here we apply this methodology to the scattering of  ${}^6\text{He}$ , treated as a three-body system of an inert  $\alpha$  particle core and two valence neutrons. A notable property of  ${}^6\text{He}$  is that none of its binary sub-systems bind, while the three-body system has a single bound state with binding energy of 0.973 MeV and total angular momentum  $j^\pi = 0^+$ . Its low-lying continuum spectrum is dominated by a narrow  $j^\pi = 2^+$  resonance, 0.825 MeV above threshold. We describe the three-body  $\alpha+n+n$  system with the

same structure model as used in Ref. [15]. The three-body Hamiltonian includes two-body interactions plus an effective three-body potential. For a given value of the maximum hypermomentum used,  $K_{\text{max}}$ , the parameters of the latter are adjusted to reproduce the ground state separation energy and matter radius (for  $j = 0^+$ ) and the resonance energy (for  $j = 2^+$ ) [15]. Calculations were performed using the codes FACE [19] and STURMXX [20]. The maximum hypermomentum in the CDCC reaction calculation was  $K_{\text{max}} = 8$ , which provides converged results for the elastic scattering of  ${}^6\text{He}$  from a heavy target [15]. The number of channels  $\beta$  was 15 ( $0^+$ ), 26 ( $1^-$ ) and 46 ( $2^+$ ). The calculated  ${}^6\text{He}$  ground state has binding energy of 0.953 MeV and a single-particle density with root mean squared (rms) radius 2.46 fm, assuming an  $\alpha$  particle rms radius of 1.47 fm.

The EC basis states have properties that are useful to describe collisions. The upper panels of Figs. 1 and 2 show the Coulomb  $B(E1)$  and  $B(E2)$  transition probabilities, respectively, as a function of the  ${}^6\text{He}$  excitation energy above threshold. The curves show the total  $B(E1)$  and  $B(E2)$  strengths (thick solid) and the contributions from the first four EC. Since the  ${}^6\text{He}(\text{g.s.})$  has  $j^\pi = 0^+$ ,  $B(E1)$  measures the electric dipole strength to  $1^-$  states, and  $B(E2)$  the quadrupole strength to  $2^+$  states. For each EC, the  $1^-$  and  $2^+$  eigenphases are also shown in the lower panels of the figures. It has been shown (see for instance Ref. [21]) that the position of the peak of the  $B(E1)$  distribution depends on the maximum hypermomentum chosen. In particular, for  $K_{\text{max}} = 10$  the maximum appears around 2 MeV, and decreases to about 1 MeV, for  $K_{\text{max}} = 20$ , for which convergence of this observable is achieved. For  $K_{\text{max}} = 8$ , which is the value used in this work, the maximum is around 2 MeV, and hence this observable is not converged. Nevertheless, as we have shown in Ref. [15], the scattering calculations are converged with this value, provided that the parameters of the three-body potential are adjusted such that the  ${}^6\text{He}$  system has the same binding energy and rms matter radius for the chosen  $K_{\text{max}}$ . In principle, the reaction calculations could be done with a higher  $K_{\text{max}}$  value, although this would turn these calculations computationally very demanding.

It is evident from Figs. 1 and 2 that there is energy localization for the EC contributions to the  $E\lambda$  strength. Also evident is that those EC with eigenphases of the largest magnitude make the maximum contribution to the  $B(E\lambda)$  at low excitation energy. This is a very appealing feature for scattering studies where, at moderate collision energies, only continuum states up to a few MeV play a significant role in the reaction process. So, for example, if excitation energies up to  $\approx 8$  MeV are strongly populated in a particular reaction, the first three or four EC should suffice to describe the relevant part of the continuum. Of course, in nuclear collisions near and above the Coulomb barrier, nuclear forces (not included in Figs. 1 and 2) will play an important role. We show below that, with nuclear interactions present, only a few EC

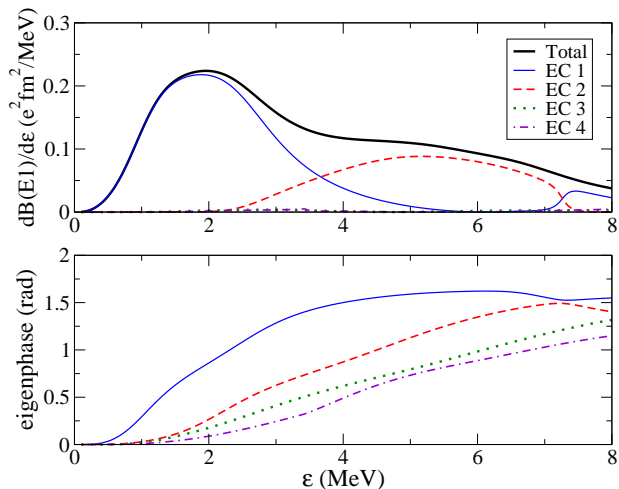


Figure 1: (Color online)  $B(E1)$  distribution (upper panel) and eigenphase shifts (lower panel) for the first few  $j^\pi = 1^-$  EC of  ${}^6\text{He}$ . The thick solid line in the upper panel is the total  $B(E1)$  distribution.

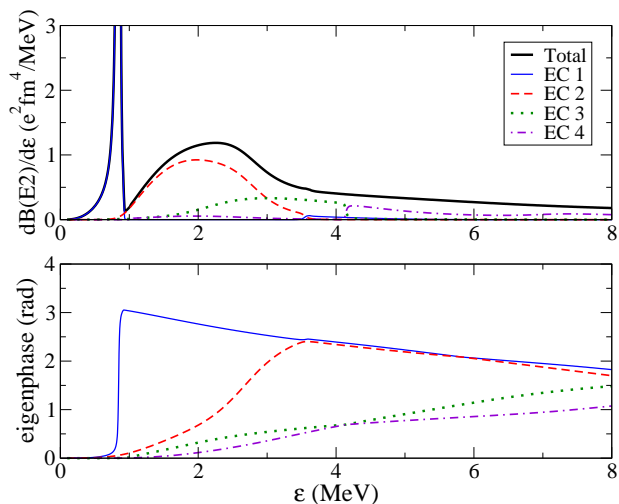


Figure 2: (Color online)  $B(E2)$  distribution (upper panel) and eigenphase shifts (lower panel) for the first few  $j^\pi = 2^+$  EC of  ${}^6\text{He}$ . The thick solid line in the upper panel is the total  $B(E2)$  distribution.

are needed for converged scattering observables.

It is also interesting to identify the dominant quantum numbers of the EC with the largest contributions to these observables. For  $B(E1)$  the most important component of EC 1 and 2 has  $l_{nn} = l_x = 0, S_x = 0$ , or a *dineutron* configuration. This dominance, could explain that previous two-body ( $\alpha + 2n$ ) model calculations of  ${}^6\text{He}$  reactions work to a limited extent, although it is well known that such simple models overestimate continuum coupling effects without parameter adjustments [22, 23]. For  $B(E2)$  the most relevant structure is the  $2^+$  resonance that corresponds to the EC 1. In this case we have a combination of three different configurations: a dineutron ( $l_x = 0, S_x = 0$ ), a cigar-like structure ( $l_x = 2, S_x = 0$ ), and a spin-triplet structure ( $l_x = 1, S_x = 1$ ).

We now compute the states of Eq. (1) and use these as the basis states for a four-body CDCC calculation using the techniques of Ref. [15]. There, a multipole expansion of the coupling potentials was developed for a three-body projectile plus target system. The weight function  $f_{\gamma j}(\kappa)$  (with  $\gamma$  instead of  $\beta'$ ) used in the superposition of states when constructing the bins Eq. (2) was taken to be unity for the non-resonant ( $0^+, 1^-,$  and  $2^+$ ) continuum and  $\sin(\delta_{\gamma j}(\kappa))$  for the resonant ( $2^+$ ) continuum. The latter provides an improved description of the resonant character.

Four-body CDCC calculations are carried out for the  ${}^6\text{He} + {}^{208}\text{Pb}$  reaction at 22 MeV, for which experimental data are available from Ref. [24]. This is one of the more demanding examples, due to (a) the importance of long-range Coulomb couplings arising from the heavy target and (b) the incident energy being near the Coulomb barrier and Coulomb and nuclear forces both playing a significant role.

Implicit in the CDCC is that the actual continuum can be truncated at a maximum excitation energy  $\varepsilon_{\max}$ , whose choice is dependent on the specific reaction and projectile energy. The convergence of the model space calculation must then be studied with respect to  $\varepsilon_{\max}$  and the number of bins assumed ( $n_{\text{bin}}$ ). For our four-body case we have, in addition, to study convergence with respect to  $n_{\text{ec}}$ , the number of EC included. The present calculations include  ${}^6\text{He}$  states with  $j^\pi = 0^+, 1^-$  and  $2^+$  and projectile-target interaction multipole couplings with order  $Q = 0, 1, 2$ . Coulomb and nuclear potentials are included. The nuclear interactions with the target used parametrized optical potentials. For  $n + {}^{208}\text{Pb}$  and  $\alpha + {}^{208}\text{Pb}$  the potentials were from Refs. [25] and [26], respectively.

The coupled equations describing the projectile-target motion were solved with the code FRESKO [27], the coupling form factors being read from external files. Partial waves up to  $J = 150$  were included and the solutions were matched to their asymptotic forms at radius  $R_m = 200$  fm. In order to check the convergence with respect to the basis size, for the different observables shown in this work, we have used five different sets that are summarized in Table I. Sets I, II, and III have the same maximum energy  $\varepsilon_{\max}$  and number of EC  $n_{\text{ec}}$ , so they are used to test the convergence with respect to the number of bins considered for each EC and  $j^\pi$ . Set IV is like set II but including the fifth EC, so it will be used to study the convergence with  $n_{\text{ec}}$ . Finally, set V is like set II but including an additional bin with  $\varepsilon = 8-9$  MeV for all EC and  $j^\pi$ , providing information on the convergence with respect to  $\varepsilon_{\max}$ .

First, we analyze the elastic scattering. Fig. 3 compares the calculated and experimental (circles) elastic differential cross section angular distributions (ratio to Rutherford). The dashed line is the one channel calculation, in which continuum states are omitted. The solid (set I), the dotted (set II), dot-dashed (set IV) and double dot-dashed (set V) lines are the full CDCC cal-

Set	$\varepsilon_{\max}$ (MeV)	$n_{ec}$	$n_{\text{bin}}(0^+)$	$n_{\text{bin}}(1^-)$	$n_{\text{bin}}(2^+)$	$N$
I	8	4	6	9	6	85
II	8	4	9	12	9	121
III	8	4	12	15	12	157
IV	8	5 (1-4,5)	(9,6)	(12,9)	(9,6)	142
V	9 (0-8,8-9)	4	(9,1)	(12,1)	(9,1)	133

Table I: Different sets of states used in this work for the four-body CDCC calculations.  $N$  is the total number of states considered (including the ground state). The parentheses are used to specify the two different bin schemes adopted depending on the EC (Set IV) or on the energy (Set V).

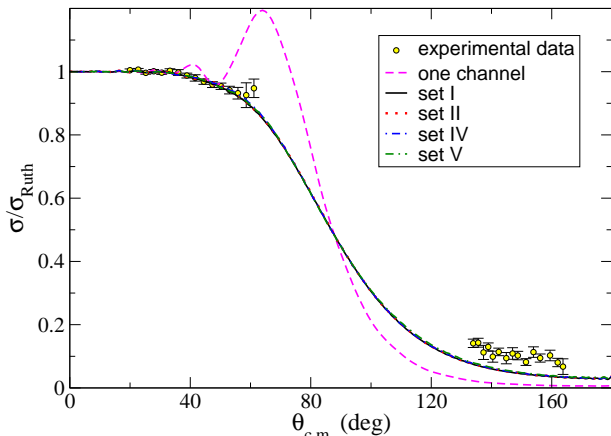


Figure 3: (Color online) Elastic differential cross section (ratio to Rutherford) in the center of mass frame for the  ${}^6\text{He}+{}^{208}\text{Pb}$  reaction at 22 MeV. See text for details. The experimental data are taken from Ref. [24].

calculations with different choices of the model space. It is remarkable that all these calculations are almost indistinguishable, showing that the elastic angular distribution is converged with set I. Also, this full four-body CDCC calculation, in contrast to the one channel calculation, describes the data fairly well. Set III is not shown since the convergence with the number of bins is already seen with sets I and II.

Solution of the CDCC coupled equations for the projectile-target S-matrix also provides predictions for breakup observables. First, Fig. 4 shows the breakup differential cross section angular distribution, summed over the excitation energy. The solid (set I), dotted (set II), dashed (set III), dot-dashed (set IV) and double dot-dashed (set V) lines are the full CDCC calculations with different choices of the model space, as in Fig 3. For this breakup observable the rate of convergence is slightly slower than for the elastic cross section, although the convergence reached with set II is fairly good.

Second, Fig. 5 shows the breakup cross section distribution, as a function of  ${}^6\text{He}$  excitation energy above breakup threshold, for each  $j^\pi$  and for each EC. This distribution is calculated by dividing the breakup cross section to each bin by its energy width. We use here set II that gives a converged result for the breakup angular

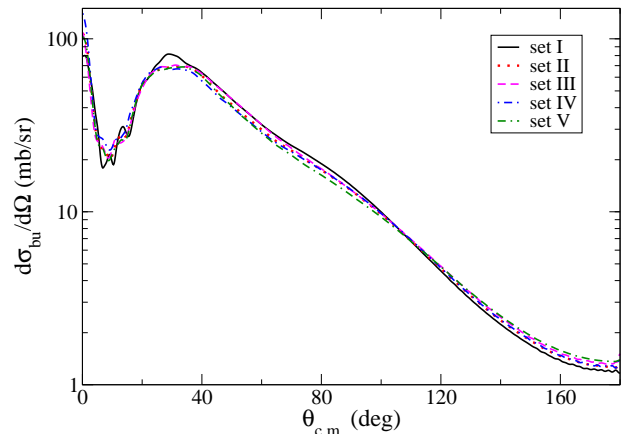


Figure 4: (Color online) Breakup differential cross section angular distribution in the center of mass frame for the  ${}^6\text{He}+{}^{208}\text{Pb}$  reaction at 22 MeV. See text for details.

distribution. As was anticipated, in all  $j^\pi$ , the contribution of each EC decreases with decreasing magnitude of its eigenphase. In particular, the contribution of the fourth EC is already small, justifying the use of a truncated calculation and  $n_{ec} \approx 4$ . We have also checked that the contribution of the fifth EC (comparing sets II and IV) changes the total breakup cross section by less than 2%. This figure also shows the importance of the dipole and resonant states. These give the largest contribution to the breakup cross section.

Collisions of loosely bound three-body projectiles with a target can be studied in the continuum-discretized coupled-channels framework. The continuum-bin discretization procedure has been formulated and used for the first time for a three-body projectile, requiring the superposition of three-body scattering states. For each three-body total angular momentum  $j$  and energy  $\varepsilon$ , scattering states are calculated for ingoing boundary conditions with quantum numbers  $\beta$ . The multi-channel S-matrix in this  $\beta$  basis, determined from the asymptotics of these states, is diagonalized to determine the eigenchannels (EC) that are ordered according to the magnitude of their associated eigenphases. We have shown that those EC with the largest eigenphases are most strongly coupled in the collision, suggesting a hierarchy of continuum states and an associated truncation scheme. This EC hierarchy allows practical CDCC calculations that extend the energy binning procedure to four-body reactions induced by three-body projectiles. The formalism has been applied to the  ${}^6\text{He}+{}^{208}\text{Pb}$  reaction at 22 MeV. The convergence of the results for elastic and breakup cross sections have been presented. Good agreement with existing elastic data for this reaction has been obtained.

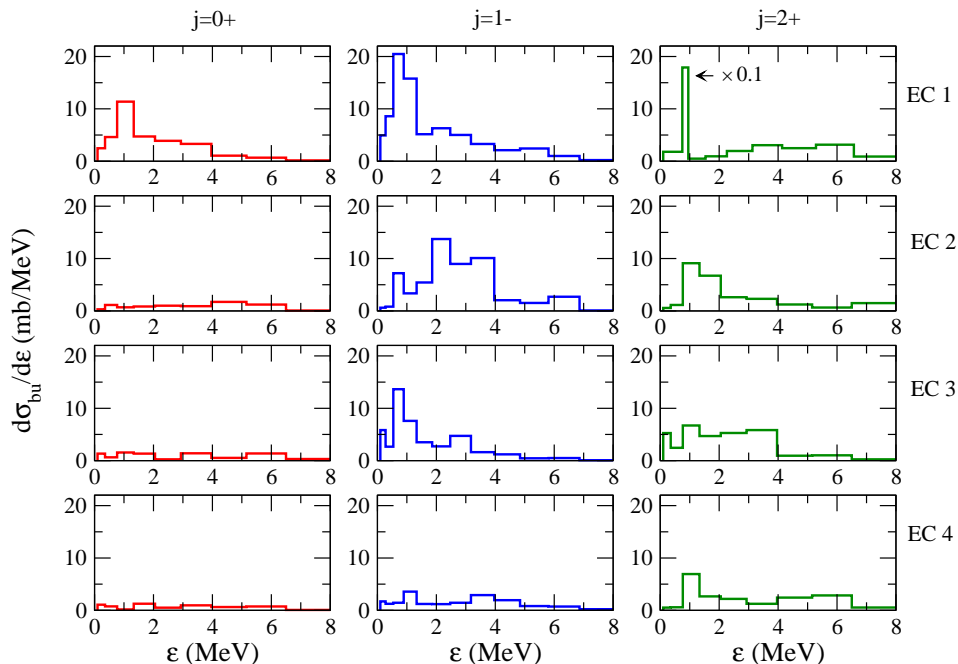


Figure 5: (Color online) Breakup cross section distribution for the  ${}^6\text{He}+{}^{208}\text{Pb}$  reaction at 22 MeV with respect to  ${}^6\text{He}$  excitation energy (over the breakup threshold) for each  $j^\pi$  and EC included in the calculation. Basis set II was used.

### Acknowledgments

We are grateful to F.M. Nunes and R.C. Johnson for useful discussions and suggestions. This work was supported in part by the FCT under the Grant POCTI/ISFL/2/275 and in part by the DGICYT under Projects FIS 2008-04189, FPA 2006-13807-C02-01, and consolider CPAN. Part of this work was performed

under the auspices of the U.S. Department of Energy by Lawrence Livermore National Laboratory under Contract DE-AC52-07NA27344. J.A.T. acknowledges the support of the the United Kingdom Science and Technology Facilities Council (STFC) under Grant EP/D003628. A.M.M. acknowledges a research grant from the Junta de Andalucía.

- 
- [1] T. Kraemer *et al.*, *Nature* **440**, 315 (2006).  
[2] I. Baccarelli *et al.*, *Phys. Chem. Chem. Phys.* **2**, 4067 (2000).  
[3] A. S. Jensen *et al.*, *Rev. Mod. Phys.* **76**, 215 (2004).  
[4] I. Muhka *et al.*, *Nature* **439**, 298 (2006).  
[5] K. Riisager, *Rev. Mod. Phys.* **66**, 1105 (1994).  
[6] P. G. Hansen, A. S. Jensen, and B. Jonson, *Ann. Rev. Nucl. Part. Sci.* **45**, 591 (1995).  
[7] M. Yahiro *et al.*, *Prog. Theor. Phys. Suppl.* **89**, 32 (1986).  
[8] N. Austern *et al.*, *Phys. Rep.* **154**, 125 (1987).  
[9] Y. Sakuragi, M. Yahiro, and M. Kamimura, *Prog. Theor. Phys. Suppl.* **89**, 136 (1986).  
[10] F. M. Nunes and I. J. Thompson, *Phys. Rev. C* **59**, 2652 (1999).  
[11] J. A. Tostevin, F. M. Nunes, and I. J. Thompson, *Phys. Rev. C* **63**, 024617 (2001).  
[12] N. C. Summers, F. M. Nunes, and I. J. Thompson, *Phys. Rev. C* **74**, 014606 (2006).  
[13] T. Matsumoto *et al.*, *Phys. Rev. C* **70**, 061601 (2004).  
[14] T. Matsumoto *et al.*, *Phys. Rev. C* **73**, 051602 (2006).  
[15] M. Rodríguez-Gallardo *et al.*, *Phys. Rev. C* **77**, 064609 (2008).  
[16] T. Egami, T. Matsumoto, K. Ogata, and M. Yahiro, *Prog. Theor. Phys.* **121**, 789 (2009).  
[17] B. V. Danilin *et al.*, *Phys. Rev. C* **69**, 024609 (2004).  
[18] P. Descouvemont, E. Tursunov, and D. Baye, *Nucl. Phys.* **A765**, 370 (2006).  
[19] I. J. Thompson, F. M. Nunes, and B. V. Danilin, *Comput. Phys. Commun.* **161**, 87 (2004).  
[20] I. J. Thompson, Unpublished. Users manual available from the author (2002).  
[21] B. V. Danilin *et al.*, *Nucl. Phys.* **A632**, 383 (1998).  
[22] K. Rusek *et al.*, *Phys. Rev. C* **72**, 037603 (2005).  
[23] A. M. Moro *et al.*, *Phys. Rev. C* **75**, 064607 (2007).  
[24] A. M. Sánchez-Benítez *et al.*, *Nucl. Phys.* **A803**, 30 (2008).  
[25] M. L. Roberts *et al.*, *Phys. Rev. C* **44**, 2006 (1991).  
[26] A. R. Barnett and J. S. Lilley, *Phys. Rev. C* **9**, 2010 (1974).  
[27] I. J. Thompson, *Comp. Phys. Rep.* **7**, 167 (1988).